

## The Continuum Interpretation for Fracture and Adhesion\*

M. L. WILLIAMS, *College of Engineering, University of Utah, Salt Lake City, Utah 84112*

### Synopsis

From the viewpoint of continuum mechanics, and particularly the energy concept of fracture, adhesive and cohesive failures are similar. The essential difference involves the interpretation of the energy required to create new (adhesive or cohesive) surface area. A simple pressurized disk test is described for measuring the adhesive value for a bonded elastomer, and an application to a debonding problem in engineering design is given.

### Introduction

At the Fifth U. S. National Congress of Applied Mechanics, the author discussed<sup>1</sup> an essential similarity between certain problems of adhesion and fracture. Considering, for example, the elastic analysis of a thin sheet in the neighborhood of a sharp geometric discontinuity such as a wedge point or crack tip, it is well known that a singularity in stress exists at the point of discontinuity and depends upon the local boundary conditions, loading, and properties of the material.<sup>2-5</sup> In the case of a central finite length crack in an infinite sheet subjected to tension, the classic Griffith problem gives a local stress variation which is proportional to the inverse square root of the distance from the crack tip.

Inasmuch as this (mathematically) infinite stress exists here for even the smallest loading, it appears that instantaneous fracture would occur and that stress analysis would not be useful for predicting a finite stress which the sheet could withstand before fracture. The essential contribution of Griffith,<sup>6</sup> however, was to develop an overall energy balance, which incorporated the integrable stress singularity, by equating the reduction in strain energy to the energy required to create new surface. The result was the prediction of a finite applied tensile stress,  $\sigma_{cr}$ , needed to initiate fracture, namely,  $\sigma_{cr} = \sqrt{2E\gamma_c/\pi a}$ , in which  $E$  and  $\gamma_c$  are the Young's modulus and energy to create new fracture surface, respectively, and  $2a$  is the finite length of the crack in the thin sheet. It is apparent, therefore that the use of the integrated energy balance neatly circumvented the question of how infinite the infinite stress need become before fracture. It furthermore

\* Based upon a lecture delivered at the Wayne State University, Polymer Conference Series, Detroit, Michigan, May 14, 1968.

suggests the way in which other problems in stress analysis having stress singularities can be attacked in order to predict a finite stress at failure notwithstanding an infinite stress at the origin of the fracture initiation.

The character of elastic stress singularities to be expected for various geometric discontinuities was investigated by Williams<sup>2,3</sup> and later applied to the specific situation of the interface between dissimilar media.<sup>7</sup> In this case too, when a crack existed along the line of demarcation of the two materials, the stress singularity was likewise singular, although not necessarily solely of the  $r^{-1/2}$  type. It subsequently became attractive to several workers in the field to inquire whether the same approach as Griffith used could be applied to predict the stress required to further separate or fracture the (adhesively bonded) interface between two different media, again notwithstanding the predicted existence of an infinite stress at the crack point for even small applied loads.

The phenomenological similarity in the two cases becomes clear. In the Griffith problem the finite length of the central crack  $2a$ , lies, say, along the  $x$  axis, with the upper and lower half planes occupied by the same material; in the second problem, the materials above and below the  $x$  axis are different. For the purposes of discussion, we shall assume the material in the lower half plane to be infinitely rigid (e.g., glass) with respect to that in the upper half plane (e.g., rubber), and assume perfect adhesion over  $|x| > a$ . The stresses at the crack ends,  $|x| = a$ , are both singular. In the first case the Griffith critical stress is the classic example of cohesive fracture and well known; in the second, the example of perfect adhesive failure is not.

Before looking into the second problem in more detail, it is pertinent to comment upon the distinction between the mechanics and chemistry viewpoints. As structured above, the mechanics approach is straightforward and consists of two parts: (1) conduct the stress analysis for an edge-bonded specimen having a central finite crack at the interface with a rigid boundary, and (2) express the incremental new surface energy generated as the crack extends. This latter part however requires interpretation.\* In the cohesive fracture problem with the same material on both sides of the extending crack Griffith used  $\Delta S = 4\gamma_c\Delta a$  as the incremental energy per unit thickness. The factor four arises because both ends of the crack are assumed to extend equally, and each end creates two new surfaces, one above and one below the crack. The specific energy  $\gamma_c$  has been subscripted to denote the value associated with cohesive failure. For adhesive failure, it would be appropriate, although not necessarily unique, to write  $\Delta S = 2\gamma_a\Delta a$

\* It should be clear that a continuum mechanics analysis does not, of itself, differentiate between a cohesive or adhesive mechanism of failure. The distinction lies in the behavior implied by using a particular one of the respective energies to create the new surface, namely  $\gamma_c$  (cohesive) or  $\gamma_a$  (adhesive). Furthermore there appears to be no direct association between the critical surface tension and the continuum mechanics analysis of the unstable infinitesimal deformation of a solid, although for special cases the critical surface stress to cause a spherical flaw to become unstable has been deduced by Williams and Schapery.<sup>8,9</sup>

to denote that only two new free surfaces are formed in the elastic material. While this leaves open to surface chemists the question of any quantitative relation between  $\gamma_a$  and  $\gamma_c$ , as long as  $\gamma_a$  is a fundamental material constant, it can be used subsequently for predicting adhesive failure in a different geometric or loading configuration. Suppressing further comment upon this point until later, let us proceed to a detailed consideration of perfect adhesion between elastic and rigid materials.

### The Elastic Rigid-Adhesive Problem

The first distinction to be drawn is that between problems for which exact or approximate solutions are available. In the first category we find two useful geometric configurations; (1) the end-bonded half plane with an interface finite crack of length  $2a$ , and (2) the end-bonded circular rod containing an interface penny shaped crack of radius  $2a$ . In both cases the discontinuity is located along the bond to the rigid boundary. The width or external rod diameter is assumed infinitely large. For these geometries of immediate concern (Fig. 1), analytical solutions for the case of uniform internal pressure in the crack are already available.<sup>10,11</sup> Without reproducing the analysis\* but merely equating the change in internal strain energy with respect to the increment in flaw enlargement,  $\Delta a$ , to the change in energy to create new adhesive surface,  $\Delta S_1 = (2\gamma_a b)\Delta a$  or  $\Delta S_2 = (2\pi a\gamma_a)\Delta a$  for problems (1) or (2), respectively, one easily deduces the results in Table I.

In principle then, either of the configurations in Table I could be used to determine  $\gamma_a$  and then verified by checking the results obtained in the other. As a practical matter there are the usual experimental difficulties, such as how one introduces uniform pressure into the crack without leakage, or how to control, repeatedly, the thickness of the adhesive coating in the various configurations. For these reasons, and to ascertain whether indeed there is a unique value of  $\gamma_a$  independent of configuration, it is useful to have as wide a range of test conditions as possible.† In the earlier paper<sup>1</sup> it was

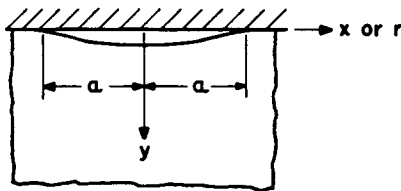


Fig. 1. Cross section geometry of a rigid-elastic bond in a sheet or rod specimen. The region  $|x| < a$  may be subjected to uniform pressure  $p_0$ .

\* The referenced results have been specialized to the case of an incompressible elastic material ( $\nu = 1/2$ ) bonded to a rigid support, in which case the oscillating character of the stress singularity<sup>7</sup> disappears and the case gives essentially the same behavior as for the homogeneous problem.

† For example, one can easily obtain similar results for the related case of a concentrated central splitting force normal to the interface.

indicated that modern computational techniques are sufficiently accurate to determine the energy gradient with crack size with sufficient accuracy, even in reasonably complicated three-dimensional problems. One could proceed to construct therefore almost any experimentally desired test configuration, although at some expense in complicating the stress analysis.

TABLE I  
CRITICAL IMPOSED PRESSURE

Configuration	$p_{cr}$	
End-bonded half-plane with line crack	$\sqrt{\frac{2}{\pi(1-\nu^2)}}$	$\sqrt{\frac{E\gamma_a}{a}}$
End-bonded rod with penny crack	$\sqrt{\frac{\pi}{2(1-\nu^2)}}$	$\sqrt{\frac{E\gamma_a}{a}}$

Returning to one of the initial points, however, it may also prove useful to inquire into the potential accuracy of approximate solutions for easily tested experimental configurations. One of the commonest ones used in adhesion evaluation is the strip peel test (Fig. 2), which has several variations as discussed and reviewed, for example, by Bikerman<sup>12</sup> and Kaelble.<sup>13</sup> While variations of this test are attractive especially for ranking purposes, its analysis is not thought to be completely satisfactory for our present purposes, although in principle it could be made so even if one resorted to numerical computations. Another example developed for cohesive failure is the cantilever split beam proposed by Obreimoff<sup>14</sup> and subsequently modified by Gilman<sup>15</sup> and Berry<sup>16</sup> for evaluating the cohesive fracture energy in thin sheets like mica (Fig. 3). In addition, the cantilever beam and the

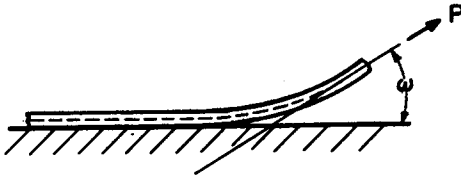


Fig. 2. External forces acting on the flexible member.

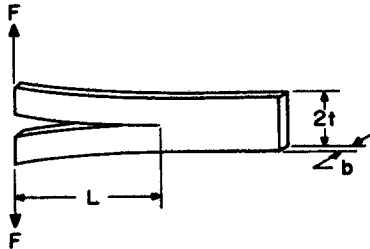


Fig. 3. Double-cantilever cleavage specimen.<sup>15</sup>

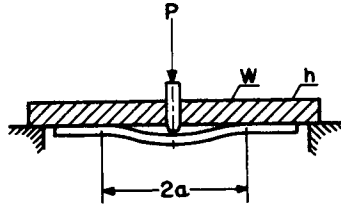


Fig. 4. Circular bonded plate with a concentrated load.<sup>17</sup>

point-loaded circular plate (Fig. 4) tests proposed by Malyshev and Salganik<sup>17</sup> seem very attractive to include in a family of practical tests for determining the adhesive energy. As a final configuration forming the series of possible geometries which can be studied, it should be noted that the previous exact solutions for the edge-bonded plane strain specimen and the rod specimen may be viewed as a limit situation as the beam or plate thickness  $h$  becomes infinite.

On viewing all the solutions in this context, both exact and approximate, and with due consideration of experimental convenience, it is proposed that Malyshev and Salganik's analysis can be supplemented by a pressurized bubble test (Fig. 4, except with uniform pressure,  $P_c$ , instead of point loading). Conceptually, this type of test is also not new, although perhaps some improvements in the analytical expression of the results can be achieved. Dannenberg,<sup>18</sup> for example, has discussed the measurement of adhesion by a blister method, which is essentially a pressurized bubble. In that case the work of adhesion was deduced from measurements of the work input,  $p dV$ , of the pressurizing fluid for application to the adhesion of paint. It may be noted, incidentally, that the consecutive detachment of the coating which he notes experimentally, is possibly related to the same "stick-slip" phenomenon frequently observed in cohesive fracture of polymers.

From the principle of energy conservation, one may write that the work done by the applied pressure moving through the virtual displacement must be balanced by the change in internal strain energy plus the change in the energy to create any new surface. Inasmuch as the change in internal energy is one-half the applied work for a linear load-deflection relation by Clapeyron's theorem,<sup>19</sup> one has

$$\frac{1}{2} \left[ 2\pi \int_0^a p_0 \delta w(r) r dr \right] = \delta(\gamma_a \pi a^2) \quad (1)$$

From plate theory, one finds that the deflection of a uniformly loaded clamped plate of radius  $a$  is given by<sup>20</sup>

$$w(r) = (1/64) (p_0/D) (a^2 - r^2)^2 \quad (2)$$

where  $D = Eh^3/12(1 - \nu^2)$  is the plate flexural rigidity, so that the energy balance yields

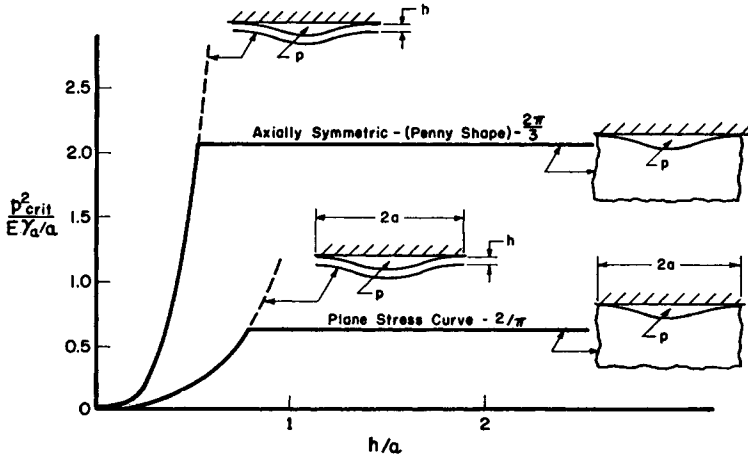


Fig. 5. Asymptotic critical pressures for rigid-elastic (incompressible) adhesive end-bonds in thin sheets (plane stress) or circular rods. The circular or slit flaw size,  $2a$ , is small compared to the width or diameter of the specimen.

$$p_{cr} = \left[ \frac{32}{3(1-\nu^2)} \left( \frac{h}{a} \right)^3 \right]^{1/2} \sqrt{\frac{E\gamma_a}{a}} \quad (3)$$

which can be compared to the rod result (Table I) of

$$p_{cr} = \left[ \frac{\pi}{2(1-\nu^2)} \right]^{1/2} \sqrt{\frac{E\gamma_a}{a}} \quad (4)$$

The comparative dependency upon  $h/a$  is to be noted.

Several of the pertinent cases have been collected in Table II for use in experimental studies. Using the pressurized crack configuration for example, one can construct the curve in Figure 5 which shows the predicted limit results for bonded rods or (plane stress) plates. By establishing these limits it is possible to bracket, with engineering accuracy, the adhesive energy value  $\gamma_a$  for a wide range of experimental configurations without having to compute explicitly the difficult transition cases.\*

As a concluding point before discussing some representative test results, it should be emphasized that the analyses of all the thin disk configurations are approximate because only beam and plate theory has been used. Actually (mathematically) infinite stresses exist at the bonded end of the beam or clamped edge of the plate at the specimen-bond interface. These are not included in the approximate analysis, and thus contribute to the potential error in adhesive energy determinations. Its degree must be ascertained. In the meantime, it is reasonable to inquire as to the degree of accuracy obtained with the simple analyses.

One may note in passing, however, that the experimental solution<sup>23</sup> achieved by Broutman and McGarry for adhesive work measurements

\* If warranted, these results can be extended to very thin plates or membranes for which the load-deflection relations are nonlinear.<sup>21,22</sup>

TABLE II  
Selected Critical Loadings for Adhesive Failure to a Rigid Medium

Geometry	Critical loading	Reference
Axially symmetric		
Bonded rod with small penny shaped crack; uniform pressure	$p_{cr}^2 = \frac{\pi}{2(1 - \nu^2)} \frac{E\gamma_a}{a}$	11
Bonded disk with small penny shaped crack; uniform pressure	$p_{cr}^2 = \frac{32}{3(1 - \nu^2)} \left(\frac{h}{a}\right)^3 \frac{E\gamma_a}{a}$	eq. (4)
Bonded disk with small penny shaped crack; central concentrated load, P	$P_{cr}^2 = \frac{8\pi^2}{3(1 - \nu^2)} Eh^3\gamma_a$	17
Thin sheets (plane stress <sup>a</sup> )		
End-loaded cantilever (length, $a$ ; width, $b$ )	15 $P_{cr}^2 = \frac{Eb^2h^2\gamma_a}{6a^2}$	17
Uniformly loaded cantilever (length, $a$ ; width, $b$ )	— $p_{cr}^2 = \frac{2Eh^3\gamma_a}{3a^4}$	—
Centrally loaded, cantilever on both ends (length, $2a$ ; width, $b$ )	— $P_{cr}^2 = \frac{8Eb^2h^2\gamma_a}{3a^2}$	—
Uniformly loaded, cantilever on both ends (length, $2a$ ; width, $b$ )	— $p_{cr}^2 = \frac{3Eh^3\gamma_a}{2a^4}$	—
Edge-bonded thin sheet. (crack length, $2a$ ); central concentrated load $P$ (lb/in) <sup>b</sup>	8 $P_{cr}^2 = 2\pi E\gamma_a a$	10
Edge-bonded sheet (crack length, $2a$ ); uniform pressure loading <sup>b</sup>	8 $p_{cr}^2 = \frac{2}{\pi} \frac{E\gamma_a}{a}$	10

<sup>a</sup> Plane strain obtained by replacing  $E$  by  $E/(1 - \nu^2)$

<sup>b</sup> Exact for plane strain and incompressible elastic medium. Estimate only for plane stress, due to oscillating type singularity; exact analysis follows from ref. 10.

might be adopted. The double cantilever-beam test, which they used, leads theoretically to a load-deflection relation containing the beam (crack) length raised to the third power when elementary beam theory is used. By actually plotting deflection per unit force versus crack length they obtained an exponent from their tests which was a constant, somewhat less than three, over a substantial range of the crack length. If this approach was applied to the pressurized disk by plotting experimental results of deflection versus pressure as a function of debonding radius, perhaps some of the uncertainty due to using Kirchhoff-Love plate theory could be eliminated.

### Experimental Results

Malyshev and Salganik<sup>17</sup> have conducted experiments using a split-beam, end-loaded cantilever, and a point-loaded circular plate (Fig. 4) using a steel-Plexiglas combination. For the circular plate configuration, they obtained the criticality relation (Table II) as

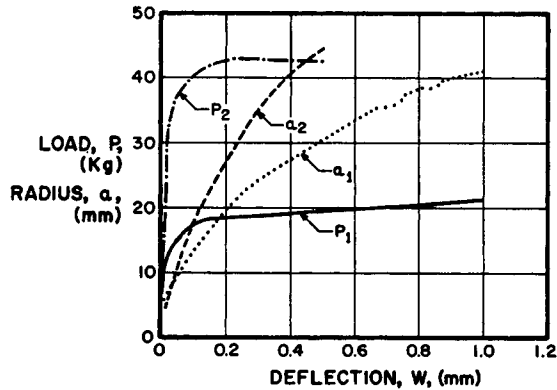


Fig. 6. Tearing force,  $P$ , and flaw radius,  $a$ , versus maximum plate deflection. Experimental data<sup>17</sup> for 3 mm and 5 mm Plexiglas sheets bonded to steel.

$$\gamma_a = p^2/32\pi^2D = (8Dw_{\max}^2/a^4) \quad (5)$$

This result indicates that if  $\gamma_a$  is a material constant, the applied force to debond the disk would remain constant while the central deflection increased proportional to the square of the disk radius. As is seen in Figure 6, reproduced from their work, there is a substantial portion of the deflection over which the applied force does remain constant. They point out that the best correlation would be expected if the deflection is smaller than the disk thickness due to limitations of the basic plate theory. This method for determining the adhesive energy  $\gamma_a$  seems very attractive and reasonably simple to obtain. It furthermore has the advantage, in contrast to the use of beamlike specimens, that bonding control need only be attained at the initial fracture front because there are no "sides" to a circular disk specimen as there are when bonding two beam strips together.

With the thought that improved sensitivity could be obtained using this same specimen but with pressurization rather than point loading, plus the fact that there results a smaller maximum deflection for the same total load, W. B. Jones has conducted some experiments using a glass-rubber combination.<sup>24</sup> Using  $\nu = 1/2$  for the Poisson's ratio of the rubber, one expects

$$\gamma_a = 9p^2a^4/128Eh^3 = 1/2 pw_{\max} = (32Eh^3/9a^4)w_{\max}^2 \quad (6)$$

It may also be noted that, in contrast to the concentrated loading, there is no necessity for the hole through which the load is introduced to remain concentric with the debonding disk for the analytic result to apply. In this respect the pressure loading is also experimentally simpler, although the fracture once started will be unstable while the concentrated load configuration is neutrally stable.

### Description of Test Results

The test vehicle for the surface energy-bond tests consisted of a glass disk having a central hole and a thin sheet of polyurethane rubber cast-bond to it.



The glass disk was of lens quality crown glass, 3.8 in. in diameter and 9.128 in. thick. A brass pressure fitting was bonded to the plate. Through it pressure was introduced, thereby causing progressive debonding (Fig. 7). Simultaneous measurements were made of the diameter of the debonded area and the imposed pressure.

The disk was prepared for casting the polyurethane by first wiping with commercial grade acetone, then with chloroform. A metal pin was then wiped with silicone vacuum grease and inserted into the hole through the brass fitting so that the end was flush with the top surface of the disk. A circular area about  $\frac{1}{2}$  in.-diameter was then thinly covered with vacuum grease to initiate unbonding. The assembly was then placed in the oven to preheat before casting.

The polyurethane rubber was made of equal volumes of Solithane 113 (a commercial polyurethane rubber available from the Thiokol Chemical Corporation) and castor oil. The components were preheated to  $140^{\circ}\text{F}$  and mixed. The mixture was degassed in a vacuum for about 10 min, then poured to desired thickness on the glass disks. The rubber was subsequently cured for about 2 hr at  $280^{\circ}\text{F}$ . The oven was then cut off and allowed to cool with the samples inside. After about 2 hr, the samples were removed and readied for testing. A metal wire was pushed through the hole to clear the flashing and to initiate unbond. The samples were attached to a regulated air supply.

Procedures usually were to pressurize the sample so that debonding initiated and propagated beyond the edges of the brass fitting so that it could be more easily observed. On some tests, however, measurements were also taken near the center of the sample. The pressure was slowly increased until debonding initiated, then was slowly decreased until the flaw line stopped propagating. Pressure values from a mercury manometer were recorded as a function of the diameter of the debond. Some typical data are shown in Figure 8.

In some tests crossed polaroids were used to enhance the contrast at the edge of the unbond.

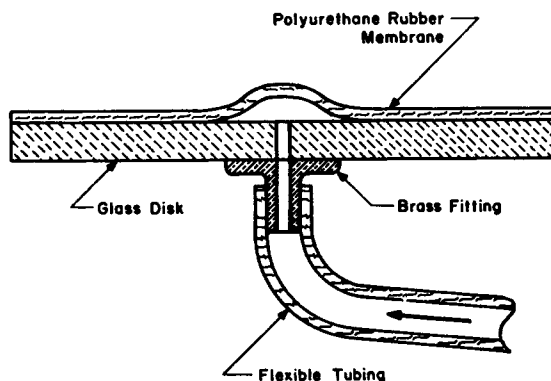


Fig. 7. Sketch of disk test specimen.<sup>24</sup>

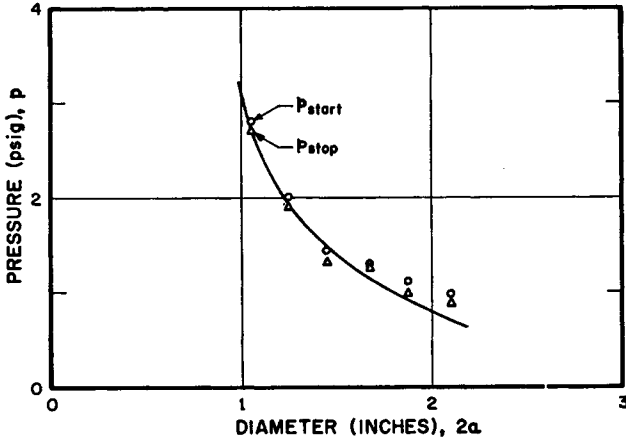


Fig. 8. Typical pressure  $p$  vs. diameter  $2a$  data for the pressurized disk.  $E = 400$  psi,  $h = 0.043$  in., giving  $\gamma_a = 1.4$  in.-lb/in.<sup>2</sup> [eq. (6)].

### Application to Complicated Geometries

With the foregoing reasonable results obtained from simple experiments it appears possible to utilize the known value of the adhesive energy in investigating adhesive failure in more complicated geometries. As an illustration, a rather sophisticated numerical analysis was used to obtain the unbonding threshold for a hollow thick-walled cylinder of polyurethane rubber cast into a glass tube and subjected to a temperature drop.<sup>1</sup>

The thermal stresses in the cylinder were computed numerically, normalized upon  $Ea\Delta T$ , and the strain energy integrated over the cylinder. Then assuming only one new free surface was created as the crack progressed along the interface, the change of potential energy  $V$  with crack length  $l$  was equated for rigid boundary displacements to the change in energy to form new surface, i.e.

$$2\pi [Ea\Delta T]^2 \delta V(\sigma_{ij}) / \delta l \Big|_{l=l_{cr}} = 2\pi b \gamma_a$$

$\sigma = \text{const.}$

leading, at criticality, to

$$Ea\Delta T_{cr} = \sqrt{\frac{E\gamma_a}{l_{cr} \delta I [(l/b)^2] / \delta [(l/b)^2] \Big|_{l=l_{cr}}}}$$

where  $I[(l/b)^2]$  is the nondimensional energy. This result for the special geometry computed is given in Figure 9.

The implications of this result appear rather interesting. Note first that for small debonding lengths, the basic variation is consistent with the usual Griffith inverse dependence upon crack length, and qualitatively that a lower temperature difference is required to propagate a larger crack than a smaller one. On the other hand, note that for  $l/b \lesssim 0.17$  the functional dependence upon the fracture length is reversed, namely that an increasing temperature is required to make a crack longer. The key to this behavior predicted by the numerical analysis is found in evaluating the rate of energy release with respect to crack length. For the shorter values of  $l_{cr}$ , the strain

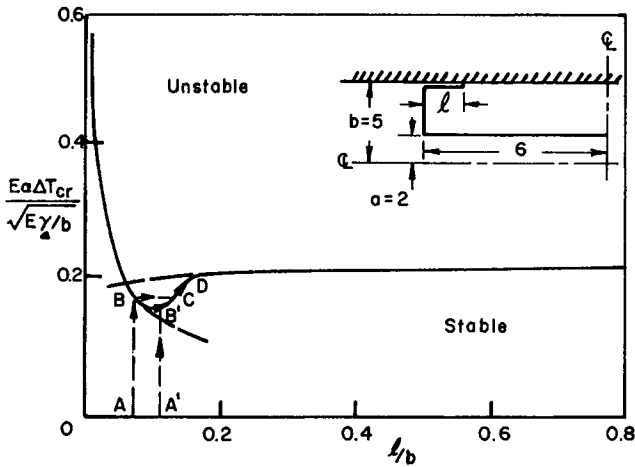


Fig. 9. Critical temperature differential as function of crack length.<sup>1</sup>

energy being released is so great that it cannot be completely absorbed by the creation of new surface, and crack instability results, as in the Griffith centrally cracked sheet. On the other hand, due to the three-dimensionality of the geometry and the existence of hoop stress, once the crack is sufficiently large, in this case  $l/b \approx 0.17$ , the energy release is just that to create the new surface—a stable growth proportional to the amount of driving force (temperature difference) present.

One therefore predicts in an elastic medium that a small crack, once started propagating by a temperature difference greater than critical for that particular length, will extend or jump to its other stable position across the “well” in Figure 9, path  $ABC$ , and proceed toward  $D$  if the temperature difference is further increased. On the other hand, if the crack begins at a larger length, path  $A'B'$ , as the temperature increases it will merely grow larger toward  $D$ , and grow in a stable fashion.

It is thus seen that the debonding characteristics could be predicted, as well as the value  $A'$  for a critical stable crack length  $l^*/b$  by using the value of adhesive energy  $\gamma_a$  from Figure 8, although the assumed independence of  $\gamma_a$  upon temperature should be verified. It is implicit, of course, that this fracture analysis also assumes the same quality of bond in both the laboratory test of the disk and the filled cylinder. While the example chosen has been deliberately more complicated than other typical engineering design problems, with, say, mechanical loading, the proposed analysis technique is thought to be direct and simple.

### Conclusions

Notwithstanding the promising success in using the continuum mechanics approach to adhesives, it is well to emphasize some of the qualifications.

\* Portions of this research were supported by a grant from the National Aeronautics and Space Administration.

First, it is not necessary from the engineering standpoint that the adhesive and cohesive energy values be associated. It suffices that they can be measured. To the extent that the bonding process in any design situation satisfactorily duplicates the process used in the specimen preparation, e.g., bond thickness, cure temperatures and pressures, and that the failure mode is the same, i.e., interfacial adhesive separation (or else cohesive failure analysis would be used), then a direct and reliable prediction can be made. Second, if subsequent experience proves the approach is practical, additional analytical refinements can be made, either by way of numerical calculations in a given configuration, or additional analytical sophistication in the way of allowing for elastic deformations in both of the bonding components, or by introducing a third interlayer representing the adhesive coating itself. Third, from the chemical standpoint it should be interesting to inquire into the possible molecular associations of the cohesive and adhesive energy values, as well as the nonisotropic boundaries, or effects of adhesive migration into the base polymer. Finally, a serious attempt should be made to reduce the peel test data, by appropriate analysis, to a form from which the specific energy values can be extracted and thus increase its quantitative value by widening the range of application of peel test data.

### References

1. M. L. Williams, *Proc. 5th U.S. Nat. Congr. Appl. Mech.* **1966**, 451.
2. M. L. Williams, *Proc. 1st U.S. Nat. Congr. Appl. Mech.* **1951**.
3. M. L. Williams, *J. Appl. Mech.*, **19**, 526 (1952).
4. M. L. Williams and R. H. Owens, *2nd U.S. Nat. Congr. Appl. Mech.*, **1954**, 407.
5. M. L. Williams and R. L. Chapkis, *3rd U.S. Nat. Congr. Appl. Mech.* **1958**, 281.
6. A. A. Griffith, *Proc. 1st Internat. Congr. Appl. Mech. Delft*, **1924**, 55.
7. M. L. Williams, *Bull. Seismol. Soc. Amer.*, **49**, 199 (1959).
8. M. L. Williams and R. A. Schapery, *Int. J. Fract. Mech.*, **1**, 64 (1965).
9. M. L. Williams, *Int. J. Fract. Mech.*, **1**, 292 (1965).
10. J. R. Rice and G. C. Sih, *J. Appl. Mech.*, **32**, 413 (1965).
11. V. I. Mossakovskii and M. T. Rybka, *PMM*, **28**, No. 6, 1061 (1964).
12. J. J. Bikerman, *J. Appl. Polym. Sci.*, **2**, 216 (1959).
13. D. H. Kaelble, *Trans. Soc. Rheol.*, **3**, 161 (1959); *ibid.*, **45** (1960).
14. J. W. Obreimoff, *Proc. Roy. Soc. (London)*, **A127**, 290 (1930).
15. J. J. Gilman, *J. Appl. Phys.*, **31**, 2208 (1960).
16. J. W. Berry, *J. Appl. Phys.*, **34**, 62 (1963).
17. B. M. Malyshev and R. L. Salganik, *Intern. J. Fracture Mech.*, **1**, 114 (1965).
18. H. Dannenberg, *J. Appl. Polym. Sci.*, **5**, 125 (1961).
19. I. S. Sokolnikoff, *Mathematical Theory of Elasticity*, McGraw-Hill, New York, 1956.
20. S. P. Timoshenko and S. Woinowsky-Krieger: *Theory of Plates and Shells*, McGraw-Hill, New York, 1959.
21. M. L. Williams, *J. Appl. Mech.*, **22**, 458 (1955).
22. L. J. Broutman and F. J. McGarry, *J. Appl. Polym. Sci.*, **9**, 589 (1965).
23. H. M. Berger, *J. Appl. Mech.* **22**, 465 (1955).
24. W. B. Jones and M. L. Williams, UTEC DO 68-019, University of Utah, February 1968.

Received March 25, 1968

Revised July 1, 1968